# Design of a large orbit gyrotron with a permanent magnet system

# Design of a large orbit gyrotron with a permanent magnet system

S. Sabchevski[a,] , T. Idehara[a], M. Glyavin[a], S. Mitsudo[a], I. Ogawa[b], K. Ohashi[c], H. Kobayashi[c]

[a]*Research Center for Development of Far-Infrared Region, Fukui University, Fukui 910-8507, Japan*
[b]*Cryogenic Laboratory, Faculty of Engineering, Fukui University, Fukui 910-8507, Japan*
[c]*Shin-Etsu Chemical Co., Ltd, Takefu-shi, Fukui, Japan*

**Abstract**

In this paper, we present results of a conceptual design study of a prospective gyro-device with a permanent magnet system and an axis-encircling electron beam. Computer-aided electron-optical design of the tube has been performed by the new version of the software package GUN-MIG named GUN-MIG/CUSP. It is based on a self-consistent relativistic physical model and is developed as a problem-oriented tool for analysis of electron-optical systems with conventional magnetron injection guns (MIG) and electron guns with field reversal (cusp guns), forming axis-encircling beams. Results of numerical experiments predict satisfactory performance of the gun which is expected to form high-quality axis-encircling electron beams with small ripple and dispersion of the velocities. Parameters of the beams (current, radius, velocity ratio, etc.) are appropriate for weakly relativistic harmonic large orbit gyrotron (LOG). The cavity was optimized for excitation of $TE_{41}$ mode at the fourth harmonic of the cyclotron frequency. The results of this feasibility study will be used as a basis for development of a novel LOG with a permanent magnet system. The target parameters of such a prospective device are frequency of generated microwave radiation about 104 GHz, output power near 1 kW and efficiency of several percent.

*Keywords:* Large orbit gyrotron; Axis-encircling electron beam; Harmonic operation

## 1. Introduction

Powerful sources of high-frequency microwave radiation are in demand for great and continuously expanding number of applications in the basic research and technology. In many respects the gyrotrons are superior to other devices due to their capability to generate microwave radiation at unprecedented power levels in the millimeter and submillimeter wavelength regions of the electromagnetic spectrum. As these sources operate near the cyclotron frequency, $\omega \approx \Omega_c$ ($\Omega_c = \eta B$, $\eta$ being the electron charge to mass ratio, and $B$ the magnetic field) or its harmonics $\omega \approx s\Omega_c$ there are two principal possibilities for further advancement towards shorter wavelengths. The first one is to use stronger magnetic fields. Nowadays, the superconducting cryomagnets are able to produce homogeneous static magnetic fields up to 10–15 T, which provides radiation of millimeter and submillimeter waves from strongly oversized interaction space in the resonant cavity. The operation and maintenance of such sources is both laborious and expensive. Due to their substantial dimensions and weight similar tubes are not suitable for a number of applications which require compact portable devices. The second possible way, which offers possibility to reduce significantly the necessary magnetic field is to use interaction at high cyclotron harmonics. Unfortunately, the high-harmonic operation is much less effective compared with fundamental operation. Moreover, the high-harmonic operation is prone to mode selection problems as a result of mode competition. These specific problems of the harmonic operation practically limit the maximum possible harmonic number to values of $s < 4$.

A relatively new and less studied scheme of interaction, known as a large orbit gyrotron (LOG) [1–4] allows the above-mentioned problem to be overcome. While in the conventional ("small orbit") gyrotron the annular electron beam consists of beamlets that have tightly wound off-axis helices with small Larmor radius in the LOG, the beam is composed of axis-encircling orbits with Larmor radius comparable to the cavity radius. An inherent feature of this device is its high-harmonic operation due to the fact that an axis-encircling beam couples effectively only with co-rotating modes having azimuthal indices equal to the resonant harmonic number [2,4]. This leads to greater mode selectivity. The mode competition can be reduced further using cavities with magnetron-like azimuthal structure [1,3]. As the harmonic numbers for such a scheme of operation can be significantly greater compared with traditional gyrotrons, the required magnetic field for gyro-devices with axis-encircling beams is greatly reduced and can be produced by a permanent magnet, thereby eliminating the need for cryogenic superconducting magnet. An important advantage of the gyro-devices with permanent magnets is that their weight and size are considerably reduced. Additionally, such portable devices are more economical and simple in operation.

Although this class of devices promises an advantageous alternative, its potential is far from being realized completely mainly due to problems with the beam quality. While the MIGs have reached a high level of perfection and effective performance, the electron guns generating axis-encircling beams still pose serious electron-optical problems which need thorough consideration in order to improve beam quality and realize the potential of gyro-devices with axis-encircling beams (such as LOG, cusptrons [3] and peniotrons).

In this paper, we present a conceptual design study of such a prospective device. The computer-aided design of the electron gun has been performed by the new version of the problem-oriented software package GUN-MIG [5] called GUN-MIG/CUSP. The code was modified to allow simulation of beam formation in electron guns employing magnetic systems with field reversal. The code is based on a self-consistent fully relativistic physical model. The simulation of the interaction between the beam and RF field has been carried out assuming Gaussian-like longitudinal field profile and using the well-known principal equations of the multimode gyrotron. Excitation of different s-harmonic $TE_{mn}$ modes with $m = s$ and maximum field amplitude of 1 T has been simulated. The results from the numerical experiments have been used to formulate the final requirements concerning beam quality and such critical parameters as beam ripple, velocity ratio, current, energy and radial dimensions of the beam. As a result of an iterative procedure both the gun and the resonant cavity were optimized in order to ensure an effective interaction between the beam and $TE_{41}$ mode.

## 2. Physical models and software

The GUN-MIG/CUSP software package is a trajectory analysis tool which traces electron orbits in combined static axisymmetric electric and magnetic fields and calculates beam parameters and electron-optical characteristics of the electron gun. It is based on a self-consistent physical model which comprises the relativistic equation of motion, Poisson's equation and relations governing extraction of beam current from different cathode regions.

In a cylindrical coordinate system $(R, \theta, Z)$ electron trajectories can be found integrating the relativistic equation of motion

$$\frac{d(m\mathbf{v})}{dt} = -e(\mathbb{E} + \mathbf{v} \times \mathbb{B}), \tag{1}$$

$$\mathbf{v} = \mathbf{i}_R \dot{R} + \mathbf{j}_\theta R\dot{\theta} + \mathbf{k}_Z \dot{Z}, \tag{2}$$

where $m$ and $e$ are the mass and charge of electron, $\mathbb{E}$ and $\mathbb{B}$ are the electric and magnetic fields. Here $\mathbf{i}_R$, $\mathbf{j}_\theta$ and $\mathbf{k}_Z$ are unit vectors. The axial and radial components of the electric field can be calculated from the electrostatic potential distribution, which obeys Poisson's equation

$$\frac{1}{R}\frac{\partial}{\partial R}\left(R\frac{\partial U}{\partial R}\right) + \frac{\partial^2 \phi}{\partial Z^2} = -\frac{\rho}{\varepsilon_0} \tag{3}$$

as well as appropriate Dirichlet and Neumann boundary conditions. Here $\rho$ is the space charge density and $\varepsilon_0$ is the permittivity of vacuum. A square-shaped grid and a five-point discretization formula are used for the solution of the boundary value problem by the finite difference method (FDM) with successive over-relaxation (SOR). The potential in an arbitrary point $(R, Z)$ is approximated by the $4 \times 4$ mesh points Lagrange interpolation [6].

The external axial magnetic field is input as a set of polynomial expansion coefficients or directly as an array produced by a separate program for magnet design. In our numerical experiments we used a field profile in the permanent magnet system designed using ELF-MAGIC code [7]. The off-axis components of the magnetic field are computed from the following expansions [8]:

$$B_Z(R, Z) = B - \frac{R^2}{4}\left(\frac{d^2B}{dZ^2} - \frac{R^2}{16}\frac{d^4B}{dZ^4} + \frac{R^4}{576}\frac{d^6B}{dZ^6}\right), \tag{4}$$

$$B_R(R, Z) = -\frac{R}{2}\left(\frac{dB}{dZ} - \frac{R^2}{8}\frac{d^3B}{dZ^3} + \frac{R^4}{192}\frac{d^5B}{dZ^5}\right). \tag{5}$$

In the current version of the code the self-magnetic field of the beam current is neglected.

The space-charge distribution is computed using a combination of the particle-in-cell method (PICM) with the area-weighted algorithm (AWA) for allocation of the charges to the mesh. The cells are defined by the same mesh which is used for the solution of the boundary-value problem. The electron beam is represented by a finite number of rays, each carrying a fraction of the total beam current. For each time step inside a given cell, the charge is deposited to the four adjacent vortices of the cell (mesh nodes) according to the AWA.

For calculation of the current extracted from the emitter the region in the vicinity of the cathode is divided into a number of small virtual diodes in which the current is governed by potential distribution and initial velocities of the thermoelectrons. It is assumed that in each virtual diode the Langmuir theory holds and the technique described in [9] is applied.

The outlined physical model of beam formation is implemented in the GUN-MIG/CUSP software package. It consists of a set of computational modules written in Fortran-77 and postprocessor program intended for systematization and visualization of the results of numerical experiments. Information is presented in the form of plots and tables on seven screens altogether and is stored in files with generic names which reflect the type of data they contain and the variant of the analyzed system. In such a way, by running the code with different initial parameters and conditions a data base containing well-structured results from various simulations is being created.

The starting current for different modes can be found from the normalized balance equation for the power of RF losses in the resonant cavity and the microwave power radiated by the electron beam. For a cavity with gaussian longitudinal profile of the field distribution the normalized beam current is given by [10]

$$\hat{I}_0 = 2.4 \times 10^{-4} I_{st} Q \left(\frac{\lambda}{L}\right)^{2s-5} (\pi\alpha)^{6-2s} \left(\frac{s^s}{2^s s!}\right)^2 \times \frac{J^2_{m-s}(kR_0)}{(v^2 - m^2)J^2_m(v)}, \tag{6}$$

where $I_{st}$ is the starting beam current (in amperes), $v$ is the eigenvalue of the operating mode $TE_{mn}$, $R_0$ is the radius of the guiding centre, $\alpha = \beta_\perp/\beta_\parallel$ is the velocity ratio, $\beta_\perp$ and $\beta_\parallel$ are the orbital and axial velocities related to the speed of light, $\lambda$ is the wavelength, $k = 2\pi/\lambda$ is the wave number, and $Q$ is the total quality factor of the resonator.

More detailed analysis of the possibility for stable single-mode operation at high cyclotron harmonics can be performed by numerical stimulation of the non-stationary processes responsible for mode excitation. For this purpose we use the well-known multimode self-consistent system of shortened equations which consists of the equations of motion and equations describing modes excitation. In this model, the dynamics of the electrons in both the external magnetic field and the field of the excited modes in the cavity is given by (see e.g. [11])

$$\frac{\mathrm{d}p}{\mathrm{d}\xi} - \mathrm{i}(\Delta + |p|^2 - 1)p = \mathrm{i}(p^{s-1}Ff\mathrm{e}^{\mathrm{i}(\Psi - s\vartheta_0)})^*, \qquad (7)$$

where $p$ is the normalized electron orbital momentum ($p(0) = 1$), $\Delta$ is the normalized cyclotron resonance mismatch, and $\vartheta_0$ is the initial phase of the electron. Here $f$ is the longitudinal profile of field amplitude. The normalized amplitude $F$ and the phase $\Psi$ obey the following equations [12]:

$$\frac{\mathrm{d}F}{\mathrm{d}t} = \frac{\omega}{2Q}(\Phi'\hat{I}_0 - s)F, \qquad (8)$$

$$\frac{\mathrm{d}\Psi}{\mathrm{d}t} = \frac{\omega}{2Q}\left[\Phi''\hat{I}_0 + 2Q\frac{\omega - \omega_{res}}{\omega_{res}}\right], \qquad (9)$$

where $\omega$ is the frequency of generated oscillations and $\omega_{res}$ is the eigenfrequency of the cavity. The complex excitation factor $\Phi = \Phi' + i\Phi''$ is given by

$$\Phi = -\mathrm{i}\frac{1}{2\pi}\int_0^{2\pi}\frac{1}{F}\int p^* f^* \mathrm{e}^{-\mathrm{i}(\Psi - s\vartheta_0)}\mathrm{d}\zeta\,\mathrm{d}\vartheta_0, \qquad (10)$$

where the integration over the reduced longitudinal coordinate, $\zeta = \beta_\perp^2 \omega z / 2\beta_\parallel c$ is performed along the total length of the interaction region. From the self-consistent solution of the Eqs. (7)–(10) the efficiency $\eta$ and the output power $P_{out}$ can be calculated from the relation

$$P_{out} = \eta U_a I_b = \left(1 - \frac{Q}{Q_{ohm}}\right)\frac{\alpha^2}{1+\alpha^2}\left[1 - \frac{1}{2\pi}\int_0^{2\pi}|p(\mu)|^2\,\mathrm{d}\vartheta_0\right]U_a I_b, \qquad (11)$$

where $U_a$ and $I_b$ are the accelerating voltage and the beam current, respectively, and $Q_{ohm}$ is the ohmic $Q$-factor of the cavity.

This briefly outlined physical model was used to simulate the LOG under consideration. Results of numerical experiments will be presented and discussed in the next section.

## 3. Results of numerical experiments

### *3.1. Results of the simulation of the gun*

Efficient operation of the gyro-devices depends critically on the quality of the beam. Therefore, although the electron gun represents only a small fraction of the device, its performance is of paramount importance for the overall efficiency of the entire system. Basic requirements, which must be satisfied by the design of the gun, are as follows: (i) Formation of high-quality beam with small velocity spread and beam ripple, which can be transported without losses to the resonant cavity. (ii) Electron beam in the cavity must be thin enough and have appropriate radius which ensures effective interaction with desired mode. (iii) Tunability of the velocity ratio by controlling the accelerating voltage. (iv) Simple electrode configuration which is not very sensitive to the fabrication tolerances and allows for easy adjustment. Specifically, the gun design is subject to the following requirements: (i) Beam current $I_b = 1.0$–$1.5$ A (cathode loading $< 8\,\mathrm{A/cm^2}$). (ii) Beam voltage $U_a \leqslant 40$ kV. (iii) Beam ripple $< 10\%$. (iv) Maximum operating magnetic field 1.0 T. (v) Velocity ratio $\alpha = 1.5$–$2.0$. (vi) Perpendicular velocity spread $< 2.5\%$.

To achieve these demands, the electron gun should be carefully designed. The choice of the configuration of the gun and magnetic field distribution is as a rule a compromise between many contradictory requirements. The advantage of simulations is enormous as it allows to explore a very large number of possible design solutions, looking for the optimal one. In search of a superior variant a lot of simulations have been carried out. The shapes and locations of the electrodes were adjusted until a beam with desired parameters was achieved. The final geometry of the electrodes that

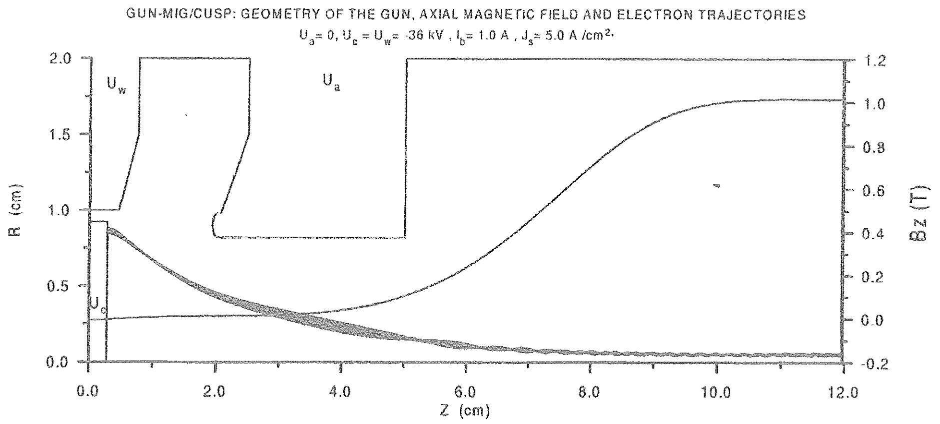


Fig. 1. Configuration of the gun, profile of the axial magnetic field produced by a permanent magnet and electron trajectories of the beam (accelerating voltage 36.0 kV; beam current 1.0 A at cathode loading 5.0 A/cm$^2$).

satisfies design requirements is shown in Fig. 1 together with the axial magnetic field distribution and electron trajectories. It can be seen in Fig. 1 that electron trajectories pass far from the surface of the anode hole. In this way, the risk of problems with beam interception is greatly reduced. The configuration of the gun is very simple as the electrode shapes are composed solely of line and arc segments. The emitter surface consists of an annular ring of 0.37 mm width and 8.635 mm average radius. At a cathode loading of 5 A/cm$^2$ (which is well within the capabilities of the dispenser barium aluminate cathodes) it gives a beam current of 1.0 A. As the cathode operates in a temperature-limited mode the beam current can be increased proportionally by increasing the loading through augmenting the temperature of the emitter.

A distinguishing feature of the gun is that it uses a gradual (instead of abrupt) reversal of the magnetic field to form an axis – encircling electron beam. The required magnetic field is produced by a permanent magnetic system, designed using the ELF/MAGIC code [7]. The first guesses concerning the field profile were obtained as a result of simulations in which the field reversal was approximated by hyperbolic tangent. The final optimal field distribution was found after numerous trials with different profiles of the axial magnetic field. Due to the fact that the magnetic field does not change so rapidly (as in the usual narrow cusps) the off-axis components can be calculated with sufficient accuracy from the paraxial expansion using Eqs. (4) and (5). This was corroborated in a number of tests comparing the results of calculation with those produced by the ELF-MAGIC code.

The radius at which electrons start, influences their final velocity components and pitch factor. The emitting area was reduced to minimize the spatial separation of the various electron trajectories and in such a way as to reduce both velocity spread and beam ripple. The ripple of different electron orbits versus their initial radial coordinate is shown in Fig. 2. It should be noted that it is easy to find (for a given electrode configuration and magnetic field profile) a point on the cathode for which electron trajectories starting there have small ripple. Unfortunately, drifting away from this optimal position electron trajectories starting from regions with greater or smaller radial coordinate have progressively increasing beam ripple.

In the increasing magnetic field the beam is compressed to the final velocity ratio and radius. The beam plotted in Fig. 1 has an average radius of 0.54 mm and thickness 0.185 mm inside the resonant cavity. The dependence of the velocity ratio ($\alpha$) on the initial radial coordinate is shown in Fig. 3. It illustrates another limitation on the dimensions of the annular emitting ring; minimization of the scattering of $\alpha$ (as well as the reduction of the scalloping of the beam) and also dictates the need to limit the percentage of variation in starting radii to a small value.

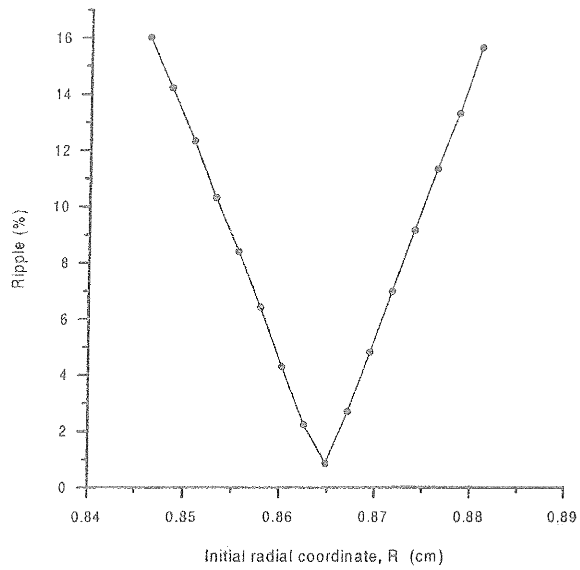


Fig. 2. Ripple of electron orbits versus their initial radial coordinate.

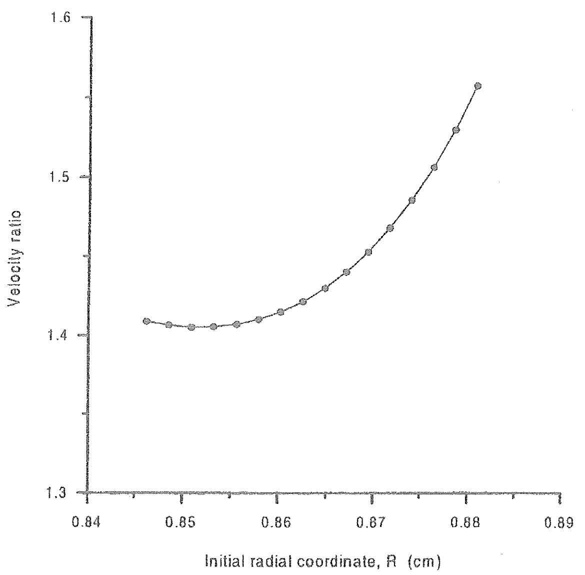


Fig. 3. Dependence of the velocity ratio ($\alpha$) on the initial radial coordinates of the electron orbits.

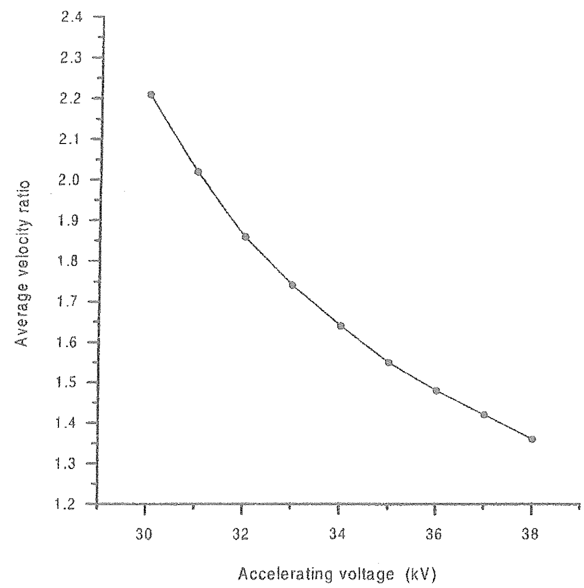


Fig. 4. Average velocity ratio versus accelerating voltage.

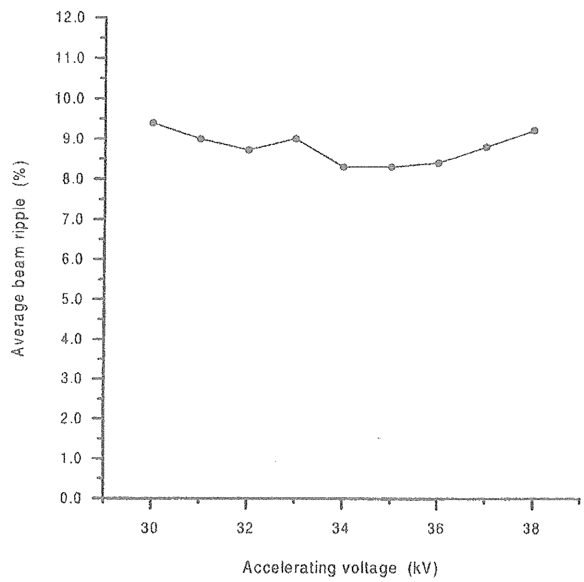


Fig. 5. Average beam ripple versus accelerating voltage.

Another key advantage of the selected configurations of the system is the ability to adjust the velocity ratio by controlling the accelerating voltage without appreciable changes of the beam quality. Fig. 4 illustrates this possibility. Simulations were performed for a range of accelerating voltages $U_a$, from 30 to 38 kV. As can be seen, the velocity ratio changes from 2.2 to 1.36, while the average ripple varies from 9.4 to 8.25% (Fig. 5). The corresponding variations of the spreads of the axial

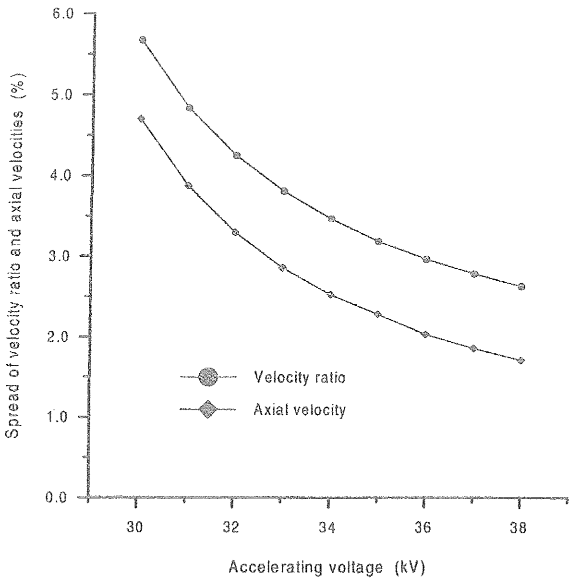


Fig. 6. Dependence of axial velocity spread and spread of velocity ratio on accelerating voltage.

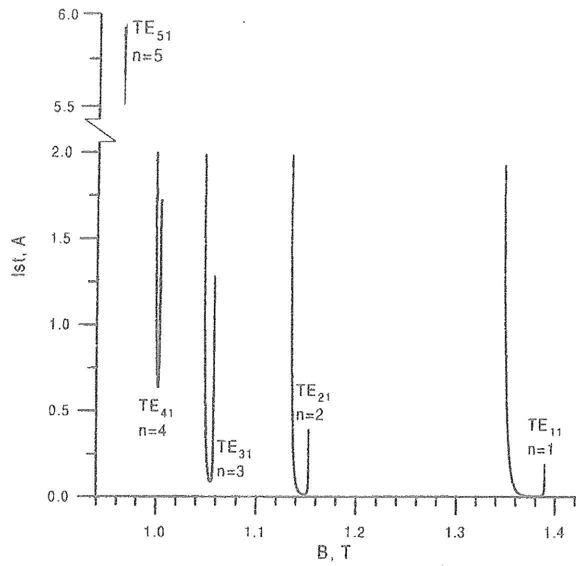


Fig. 7. Starting currents ($I_{st}$) versus magnetic field ($B$) for $TE_{m,1}$ modes ($U_a = 31$ kV, $\alpha = 2.0$, $L = 50$ mm, $R_{cav} = 2.39$ mm, $R_b = 0.54$ mm).

velocities and the velocity ratio with the change of the accelerating voltage are shown in Fig. 6.

The results of the computer simulation predict a satisfying electron-optical performance of the designed electron gun. It is expected that the gun will generate axis-encircling beams with small ripple, low-velocity spread and appropriate beam parameters (current, velocity ratio, radius in the cavity) suitable for compact, low-energy gyro-devices with axis-encircling orbits.

### 3.2. *Results of simulation of the resonant cavity*

As initial data for simulation of the resonant cavity we used beam parameters obtained from the trajectory analysis of the gun. In order to identify the possible candidate for excitation by beams of low voltage ($<40$ kV) and low currents ($<2$ A) different modes were considered. It follows from the calculations that the best separation of the resonant magnetic field can be realized for $TE_{m,1}$ modes. The starting currents for several $TE_{m,1}$ modes versus magnetic field are presented in Fig. 7. It can be seen that the increase of the harmonic number has two distinct consequences. First, it leads to higher minimum starting currents and, second, for higher harmonics the resonant lines in Fig. 7 become narrower. It is obvious, that for the given beam parameters and maximum value of the magnetic field, the highest mode which can be excited is $TE_{41}$ at $s = 4$. Therefore, this mode was selected as the operating one in the prospective LOG under consideration.

The strong dependences of the minimum starting currents for excitation of $TE_{41}$ mode on the accelerating beam voltage (at fixed velocity ratio) and on the velocity ratio (at fixed beam voltage) are shown in Figs. 8 and 9, respectively. Taking into account the imposed limitations on the beam energy, from these plots it follows that electron beams with higher pitch factor are required in order to keep the starting currents below the beam currents provided by the gun. Another parameter, which strongly influences the starting current, is the length of the resonant cavity (Fig. 10). On the one hand, in order to reduce the starting current, the length of the interaction area must be increased. On the other hand, as can be seen in Fig. 10, this results in a significant increase of the fraction of ohmic losses in the total losses (given by the ratio between the total $Q$-factor ($Q$) and the ohmic one ($Q_{ohm}$). Thus, the choice of the cavity length is always

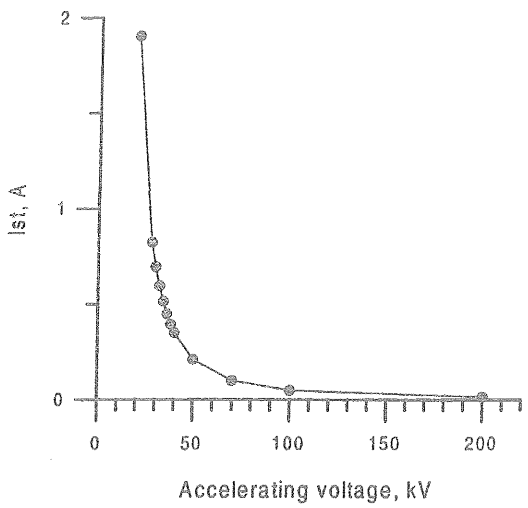


Fig. 8. Minimum starting current ($I_{st}$) for excitation of $TE_{41}$ mode as a function of accelerating voltage ($\alpha = 2.0$, $L = 50$ mm, $R_{cav} = 2.39$ mm, $R_b = 0.54$ mm).

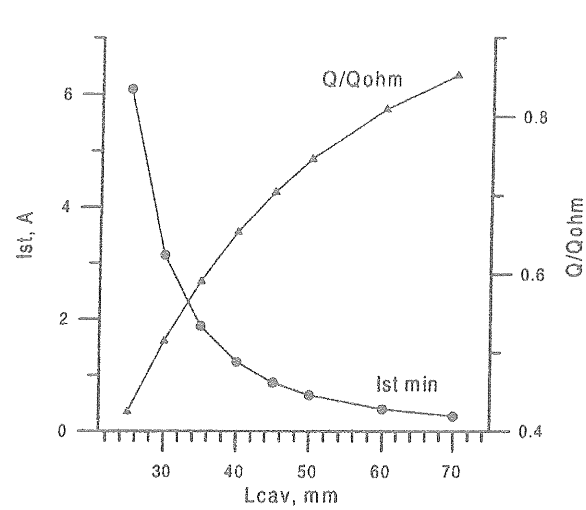


Fig. 10. Minimum starting current ($I_{st}$) and portion of ohmic losses ($Q/Q_{ohm}$) for $TE_{41}$ mode versus cavity length $L_{cav}$ ($U_a = 31$ kV, $\alpha = 2.0$, $R_{cav} = 2.39$ mm, $R_b = 0.54$ mm).

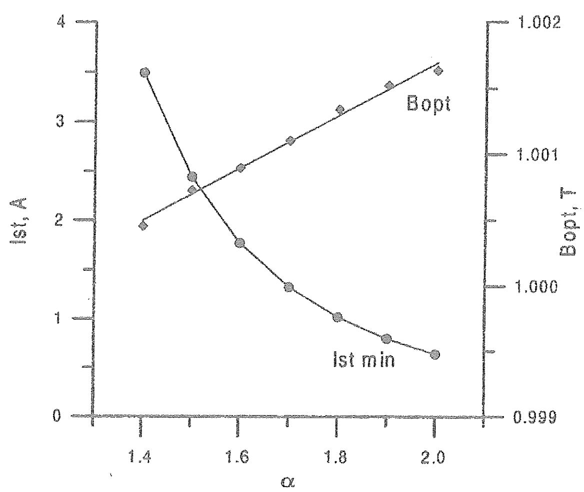


Fig. 9. Minimum starting current ($I_{st}$) and optimum magnetic field ($B_{opt}$) for $TE_{41}$ mode versus velocity ratio ($U_a = 31$ kV, $L = 50$ mm, $R_{cav} = 2.39$ mm, $R_b = 0.54$ mm).

a compromise between several competing requirements. It should be noticed that the longitudinal extent of the resonator is limited also by the fact that it is difficult to maintain the synchronism condition between the beam and RF field over long distances. Additionally, there are technological problems to produce permanent magnets with a long uniform region (top-flat region) as well as to manufacture long cavities of small radius. Taking into account all these considerations the length of the cavity was chosen to be 50 mm.

The dependence of the starting current on the accelerating voltage for the chosen dimensions of the cavity is shown in Fig. 11. The values of the velocity ratio corresponding to different voltages are those obtained from the simulation of the gun. This plot illustrates the increase of the starting current with increasing the beam voltage due to the decrease of the velocity ratio. A sufficient excess of the beam current over the starting current can be obtained for accelerating voltages in the range 30–35 kV at nominal cathode loading.

Another important observation concerns the optimum value of the magnetic field in the resonator (Fig. 11). It is clear that along with the permanent magnet, which produces the nominal required value of the magnetic field, additional coils for adjustment and fine tuning of the magnetic field in the resonator are required.

Results from computer simulation of the mode excitation using the self-consistent physical model (Eqs. (7)–(10)) are presented in Figs. 12 and 13. In Fig. 12 the time evolution of the output power is shown. Although the neighbouring modes were

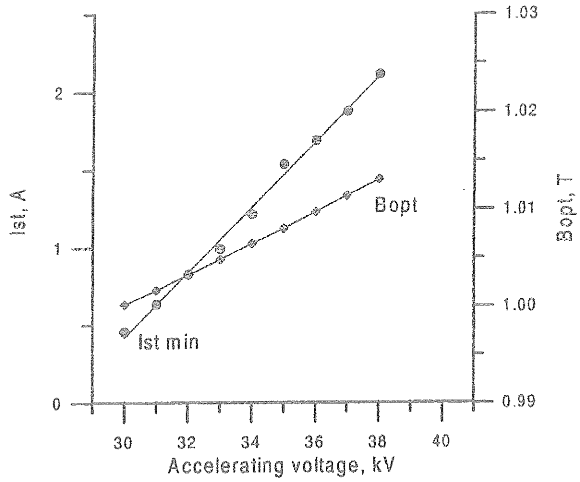


Fig. 11. Minimum starting current ($I_{st}$) for $TE_{41}$ mode and corresponding values of the optimal magnetic field ($B_{opt}$). For each point of the plot velocity ratio obtained from simulation of the electron gun is used.

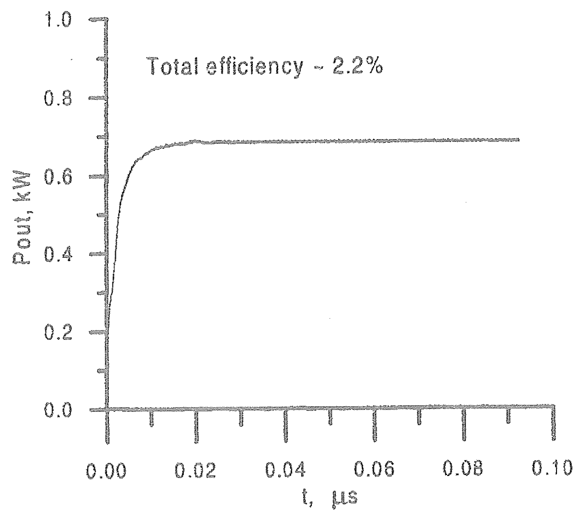


Fig. 12. Time evolution of the output power ($U_a = 31\,kV$, $I_b = 1.0\,A$, $\alpha = 2.0$).

taken into account, the results of numerical experiments indicate that they are not excited and a single-mode operation takes place. The energy spectrum of the spent electron beam ($S(W)$ versus $W/W_0$, where $W_0$ is the initial energy) with an initial transverse velocity spread of 1.0% is shown in Fig. 13. It can be seen that most of the electrons

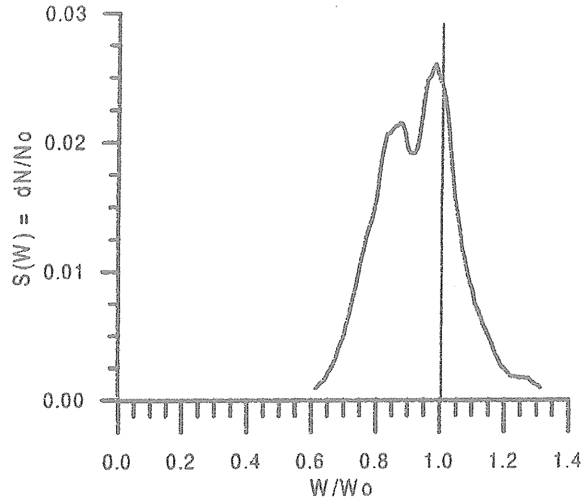


Fig. 13. Energy spectrum ($S(W)$) of the electron beam after interaction ($W$ — energy of the electrons after interaction, $W_0$ — initial energy, $dN$ — number of particles with energy $W$, $N_0$ — total number of particles).

have given part of their energy to the field but the total efficiency is low (about 2.2%) due to the considerably high ohmic losses and small excess of the operating current over the threshold starting current.

## 4. Conclusion

Using the new version of GUN-MIG software package an initial electron-optical design of a new gun with permanent magnetic system generating axis-encircling beams has been performed. The presented results indicate the feasibility of a weakly relativistic LOG with output power nearly 1.0 kW and frequency of the generated radiation 104 GHz. The main advantages of such a device would be the absence of a cryogenic system, small weight and dimensions and a simple and compact power supply. In combination, the predicted output power and frequency of the radiation makes such a tube suitable for different applications in basic research and technology. Additionally, it is hoped that such a device will be an excellent tool for accumulating the knowledge and experience needed for the development of more efficient gyro-devices with more powerful axis-encircling beams. The permanent magnetic system is under construction now. After its completion, the final electron-optical design of the electron gun will be accomplished using the real (measured) magnetic field distribution as well as additional coils for its adjustment.

## Acknowledgements

This work was performed as a part of an ongoing joint research project between the Research Center for Development of Far-Infrared Region at the Fukui University, Japan and Laboratory of Physical Problems of Electron Beam Technologies at the Institute of Electronics of the Bulgarian Academy of Sciences, Sofia, Bulgaria in a collaboration with the Institute of Applied Physics at the Russian Academy of Science, Nizhny Novgorod, Russia. The work was partially supported by Grant-in-Aid from the Ministry of Education, Science and Culture of Japan.

## References

[1] Lau YY, Barnett LR. Int J Electron 1982;53:693–6.
[2] McDermott DB, et al. Phys Fluids 1983;26:1936–41.
[3] Uhm HS, Kim CM, Namkung W. Phys Fluids 1984;27:488–98.
[4] Bratman VL, et al. IEEE Trans Plasma Sci 1999;27: 456–61.
[5] Sabchevski SP, Mladenov GM, Idehara T. Int J Infrared Millimeter Waves 1999;20:1019–35.
[6] Ximen J. Aberration theory in electron and ion optics. In: Hawkes PW, editor. Advances in electronics and electron physics. London: Academic Press, 1986; Suppl 17.
[7] ELF Corp. Japan, The Software ELF/MAGIC (Magnetic Field Analysis by Integral Computation).
[8] Hawkes PW, Kasper E. Principles of electron optics: Basic geometrical optics, vol. 1. London: Academic Press, 1989.
[9] Sabchevski SP, et al. Nucl Instr and Meth 1996;A381: 185–93.
[10] Nusinovich GS, Erm RE, Elektronnaya Tekhnika; Seria I Elektronika SVCh 1972;8:55–60 [in Russian].
[11] Nusinovich GS. Int J Electron 1988;64:127–35.
[12] Zapevalov VE, Nusinovich GS, Izv VUZov Radiofiz 1984;27:117–120 [in Russian].